Eur. J. Mech. B/Fluids, **17**, n° 4, 561–569, 1998

Elliptic instability in two-sided lid-driven cavity flow

H. C. KUHLMANN *, M. WANSCHURA, H. J. RATH

ABSTRACT. – The recently discovered concentration of vorticity in slender vortex tubes in turbulent flow fields has motivated the investigation of a class of vortices with elliptical streamlines. As a prototype of this flow, long vortices confined in a rectangular cavity and driven by tangentially moting walls are studied. These vortices are characterized by a large rate of plane strain at the core. The quasi-two-dimensional flow is found to be unstable at small Reynolds numbers, if the eccentricity of the streamlines, i.e. the strain rate, is sufficiently large. The three-dimensional supercritical flow is found to be steady with a wavelength of the order of the vortex core diameter. The flow pattern appears in the form of rectangular cells that are very robust. Good agreement between experiment and numerical calculations is obtained. It is argued that the instability found is due to the elliptic instability mechanism.© Elsevier, Paris

1. Introduction

The dynamics of vortices is an important topic in fluid mechanics. Vortices are most commonly created by vortex shedding behind bluff bodies or by the roll up of vortex sheets created by shear layers. Even for fully developed turbulent flow it has been confirmed that the vorticity is mainly concentrated in thin vortex tubes which have been termed the *sinews* of fluid motion (Küchemann, 1965, and Moffatt *et al.*, 1994), since the vortex tubes connect the larger eddies (*muscles*) having much weaker vorticity. Due to the asymmetric strain present in the turbulent flow the concentrated vortex tubes become slightly elliptical in shape (Moffatt *et al.*, 1994). On the other hand, viscous vortices with elliptical streamlines can become unstable to three-dimensional perturbations (Landman and Saffman, 1987). This so-called elliptic instability provides a very efficient means of vorticity redistribution in the turbulent flow field, although vortex stretching may act stabilizing (Le Dizès *et al.*, 1996).

To date, only few experiments on the elliptic instability are available (*see*, e.g. Gledzer and Ponomarev, 1992, and references cited therein). Typically, a liquid filled cylinder with an elliptical cross section is suddenly stopped from rigid body rotation. Thereafter, the fluid is forced to flow along elliptical streamlines and for sufficiently high initial rotation rate the quasi-two-dimensional motion becomes unstable to a three-dimensional flow that appears in the form of cells. This type of flow, however, is intrinsically unsteady making precise measurements difficult. Similarly, the three-dimensional instability of free shear layers or the three-dimensional decay of Tollmien-Schlichting waves leading to the so-called Λ-vortices (Herbert, 1988) which are believed to be initiated by the same mechanism are spatially developing flows.

In contrast to spatially or temporally developing flows, we consider a closed system which allows for steady quasi-two-dimensional flows with elliptical streamlines. This flow enables the direct observation of the elliptical instability and the evolution to a saturated, steady, and well-defined three-dimensional flow of finite amplitude. Moreover, higher instabilities, e.g. the transition to time-periodic three-dimensional flow, are easily observable.

ZARM, Universität Bremen, 28359 Bremen, Germany
* Correspondence and reprints. E-mail: kuhl@zarm.uni-bremen.de

0997-7546/98/04/© Elsevier, Paris

We report on experiments and numerical calculations. A more complete account of the result has been published recently (Kuhlmann *et al.*, 1997).

2. Experimental

The system under consideration is a nearly rectangular cavity shown in Figure 1. The fluid motion is induced by moving two facing walls tangentially in opposite directions ($\pm\vec{e}_y$). The moving walls are realized by two chrome-plated metal cylinders of radii R_i ($i = 1, 2$) rotating with circular frequencies Ω_i. All other walls are stationary. The flow can be observed through a transparent lid (at $y = 1/2$) as well as through the two stationary sidewalls (at $z = \pm 1/2$) which are machined to match the radii of the rotating cylinders. Both the lid and the sidewalls are made from Plexiglas. The rotating cylinders are driven via tooth belts by two computer-controlled permanent-magnet synchrone motors. The test liquid was Bayer 'Baysilone M20' silicone oil of kinematic viscosity $\nu = 0.236$ cm^2 s^{-1} at temperature $T = 20$ °C. The temperature in the liquid bath was permanently measured to periodically update the two Reynolds numbers

$$\mathrm{Re}_i = \frac{\Omega_i R_i h}{\nu}, \qquad i = (1, 2), \tag{1}$$

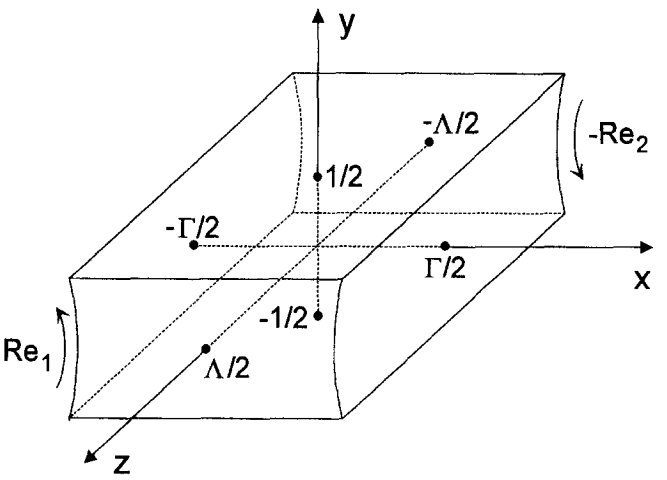

Fig. 1. – Geometry and coordinate system of the cavity.

in order to keep them at their prescribed values. Here we use the height $h = (29.0 \pm 0.1)$ mm as the length scale. The geometry is then defined by the two aspect ratios

$$\Gamma = \frac{d}{h} = 1.96 \pm 0.05, \tag{2}$$

and

$$\Lambda = \frac{l}{h} = 6.55, \tag{3}$$

where l is the length of the cavity in z-direction and d the mean value of the horizontal distance between the two cylinder surfaces. The tolerance given in (2) is due to the slight curvature of the moving walls.

3. Numerical methods

Parallel to the experiments numerical calculations have been carried out to compute the two-dimensional flows in the limit $\Lambda \to \infty$, i.e. the flow in the absence of stationary rigid lateral walls. These flows have been calculated using a mixed finite-difference Chebyshev collocation method that has been described in Kuhlmann *et al.* (1997) and Wanschura *et al.* (1995).

The linear stability of the two-dimensional basic flows with respect to arbitrary three-dimensional perturbations was investigated by a linear stability analysis. The form of the neutral modes is

$$(u,\, v,\, w,\, p)\,(x,\, y,\, z) = (\hat{u},\, \hat{v},\, \hat{w},\, \hat{p})\,(x,\, y) \times e^{\sigma t - ikz} + \text{c.c.}, \tag{4}$$

where k is the wavenumber in z-direction and σ is the growth rate which is generally complex. The resulting two-dimensional linear differential equations are discretized with the same method as used for the basic flow. The associated generalized eigenvalue problem is then solved by inverse iteration. In order to analyze the energy transfer between the two-dimensional basic flow and the three-dimensional disturbances the different integrals of the Reynolds-Orr energy equation

$$\partial_t E_{kin} = -D + \sum_{i=1}^{4} I_i \tag{5}$$

are calculated *a posteriori* using Simpson's rule and finite differences for the derivatives. Here, D is the rate of dissipation and I_i denotes the terms describing the interaction of the disturbance flow with the base state which is indicated by a zero subscript

$$D = \int_V (\nabla \vec{u})^2 \mathrm{d}V, \tag{6}$$

$$\sum_{i=1}^{4} I_i = -\int_V \left\{ u^2 \frac{\partial u_0}{\partial x} + uv \frac{\partial u_0}{\partial y} + vu \frac{\partial v_0}{\partial x} + v^2 \frac{\partial v_0}{\partial y} \right\} \mathrm{d}V. \tag{7}$$

4. Results

We restrict our attention to the case $\mathrm{Re}_1 = \mathrm{Re}_2$. Then both sidewalls move with equal velocities in opposite directions and the Reynolds number is $\mathrm{Re} = \mathrm{Re}_1 = \mathrm{Re}_2$. The two-dimensional flow in the limit $\Lambda \to \infty$ depends on the Reynolds number and the cross sectional aspect ratio Γ. For the finite experimental aspect ratio $\Lambda = 6.55$ three-dimensional end effects are always present in the flow. We have not quantified the magnitude of the three-dimensional effects. The following observations, however, indicate the quasi-two-dimensional character of the flow in the bulk except for layers of thickness $|\Delta z| \lesssim 1$ away from the sidewalls at $z = \pm\Lambda/2$. First, the streaklines of the subcritical bulk flow under investigation in thin layers parallel to the $(x,\, z)$-plane appear parallel to the x-axis. Second, the streaklines taken at cross sections in the bulk with $z = \text{const.}$ are indistinguishable from numerically calculated two-dimensional streamlines. From these observations we conclude that the base flow in the bulk is well approximated by the numerically calculated pure two-dimensional flow. Note that a similar side wall effect is present in finite-length Taylor-Couette experiments and simulations (cf. Alziary de Roquefort and Grillaud, 1978). Another indication in support of this assumption is provided by

the numerically predicted linear stability properties of the exactly two-dimensional flow being in close agreement with those of the experimental quasi-two-dimensional flow (section 4.2). For a more detailed discussion of the end effects, *see* Kuhlmann *et al.* (1997).

4.1. Steady two-dimensional flow

When the Reynolds number is small the flow in the cavity is unique. For sufficiently high Reynolds numbers, however, two different two-dimensional flow states exist depending on the aspect ratio Γ. The parameter range of non-uniqueness is the triangular shaped region made up by the solid lines in Figure 2. It is approximately given by the relations

$$\mathrm{Re} \gtrsim \mathrm{Re}_0^{(0-)} := 310\,(\Gamma - 1.2) \qquad \text{and} \qquad \Gamma \gtrsim 2. \tag{8}$$

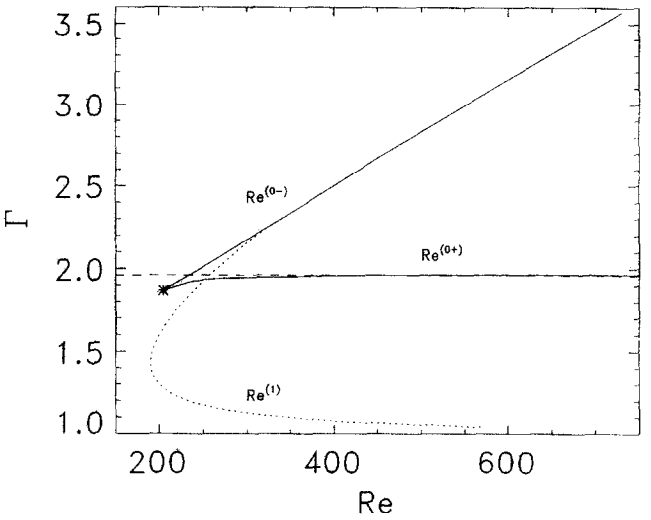

Fig. 2. – Solid lines: Upper existence Reynolds number $\mathrm{Re}_0^{(0+)}$ for the two-vortex state and lower existence Reynolds number $\mathrm{Re}_0^{(0-)}$ for the cat's eye state. The linear stability boundary $\mathrm{Re}^{(1)}$ of the cat's eye state is indicated by the dotted line. The dashed line corresponds to the experimental aspect ratio $\Gamma = 1.96$

One type of flow consists of two independent vortices adjacent to each moving lid. We shall call it *two-vortex flow*. The flow within each vortex is very similar to that of a single vortex in the well-known one-sided lid-driven cavity flow problem (*see*, e.g. Koseff and Street, 1984). At high Reynolds numbers the streamlines in the bulk take a circular shape (Batchelor, 1956). This flow state will not be considered in the following.

In addition to the two-vortex state another flow state exists under conditions (8). We shall call it the *cat's eye state*, because for the experimental aspect ratio the flow structure consists of two small recirculation regions with the same sense of circulation embedded in a globally circulating flow over the whole cavity (*Fig.* 3). The outermost streamlines of the two internal vortices form a separatrix with a hyperbolic stagnation point in the center. The topology of the two-dimensional flow depends of the Reynolds numbers and the aspect ratio Γ. Note that this particular streamline pattern is only a special case of a class of flows which are generally characterized by a significant amount of fluid being accelerated by both moving walls in contrast to the two-vortex state in which each vortex is mainly driven by the moving wall to which it is attached. The streamline patterns of the cat's eye states develop continuously along the solution manifold. When the Reynolds number is increased

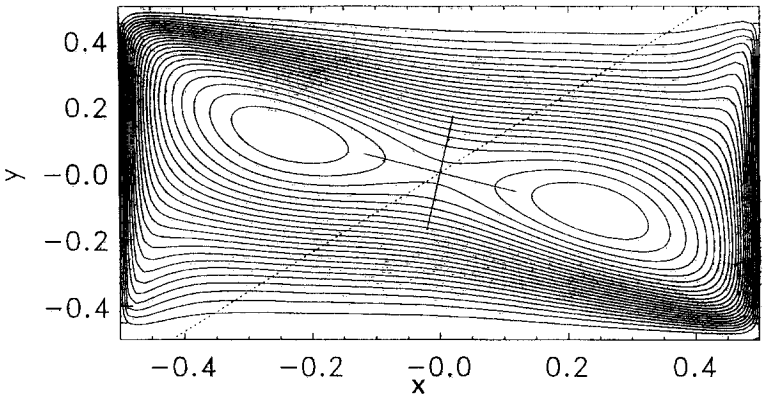

Fig. 3. – Streamlines of the two-dimensional flow for Re = 257 and $\Gamma = 1.96$.
The streamlines agree very well with the experimental ones at $z \approx 0$. The x-axis has been scaled by d.

($\Gamma = 1.96$), for instance, the size of both recirculation zones within the separatrix shrinks to zero and the hyperbolic stagnation point transforms smoothly into an elliptic stagnation point. Nevertheless, we shall still refer to this state as the cat's-eye state. A change of the topology of the flow can also be due to a change of the geometry, i.e. the aspect ratio Γ. This has been demonstrated recently by Kelmanson and Lonsdale (1996) for Stokes flow in a two-sided lid-driven cavity. It is obvious, in particular, that the internal hyperbolic stagnation point must vanish for $\Gamma \to 1$.

It turns out that the cat's eye flow, if it exists, is preferred over the two-vortex flow in the present experiment ($\Gamma = 1.96$) (*Fig.* 3). The existence and the different topologies of this state can be understood in terms of the following arguments. In the cat's eye state opposing wall jets are generated due to inertia near both downstream corners of the movings walls. Each wall jet remains confined to the stationary wall and reaches the respective opposite moving wall. Here, the fluid is accelerated again to be released from the boundary layer on the moving wall into the opposing wall jet. The corresponding streamlines for large Γ and high Reynolds number take the form of a single stretched vortex located in the center of the cavity (elliptical stagnation point). An example is shown in Figure 4. For lower Reynolds numbers near the existence boundary (8) the wall jets do not have as much inertia and the boundary layers become much thicker. As a consequence the opposing jets meet and split in the center of the cavity, one part of each jet forming the respective internal recirculation zone, the other parts forming the global circulation.

The flow near the center of the cavity can be described locally by a streamfunction

$$\psi(x, y) = \frac{1}{2}\left((\gamma - \varepsilon)\, x^2 + (\gamma + \varepsilon)\, y^2\right), \tag{9}$$

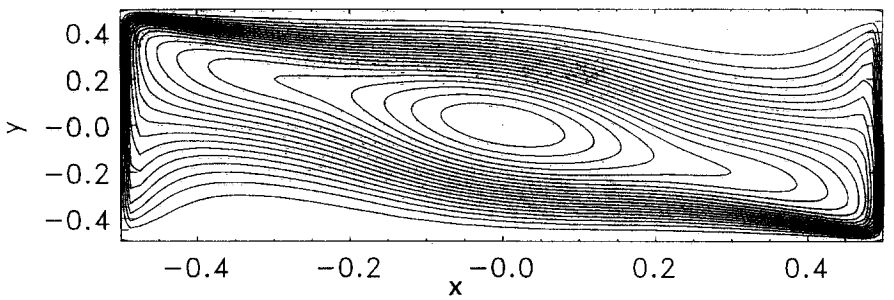

Fig. 4. – Streamlines of the two-dimensional flow for Re = 800 and $\Gamma = 3.3$ (the x-axis has been scaled by d). The flow is linearly unstable.

where $\gamma > 0$ is the rotation rate, $\varepsilon > 0$ is the rate of strain, and the coordinate system is slightly rotated (cf. *Fig.* 3). A cat's eye structure corresponds to $\varepsilon > \gamma$, indicating the dominating straining motion in the center $x = y = 0$ for the cat's eye flow.

The two-dimensional flow driven by the wall jets, i.e. the cat's-eye flow, is unstable to three-dimensional perturbations at high Reynolds numbers (*Fig.* 2). It is experimentally observable only in a small range of parameters, for which the streamlines take the shape of cat's eyes.

4.2. Three-dimensional instability of the cat's-eye flow

The near critical flow in the present experiment (cf. *Fig.* 3) is characterized by a finite region near the central stagnation point where it is hyperbolic. The flow near stagnation points of the eyes is locally elliptic. Finally, the flow circulating outside the separatrix has an elliptic character in the sense that it is subject to strain so that the streamlines are not circular. Thus the flow is clearly of a mixed type.

Stability results are available for linear flows, i.e. flows that are either elliptic or hyperbolic and of infinite extent. Infinitely extended hyperbolic stagnation point flow is always unstable in ideal fluids (Lifshitz and Hameiri, 1991) as well as in viscous fluids (Lagnado *et al.*, 1983). Likewise, elliptic stagnation point flow for which the plane strain rate is larger than the rotation rate is unstable in ideal fluids (Pierrehumbert, 1986; Bayly, 1986; and Waleffe, 1990). Landman and Saffman (1987) have shown that the viscous flow with elliptical streamlines in an unbounded domain is also unstable, albeit only for Reynolds numbers larger than some finite value. Moreover, the wavenumber k of the most dangerous mode, which can be arbitrary large in ideal fluids, is finite in the viscous case.

In spite of these results for linear flows, no results are available for mixed flows as in the present experiment. It is useful, however, to compare the linear stability results and instability mechanisms for the present case with those of the linear flows. For the present cavity flow we find that the cat's eye flow can be unstable at rather low Reynolds numbers. The critical three-dimensional mode is always stationary. For the experimental aspect ratio $\Gamma = 1.96$ the instability occurs at $\mathrm{Re}_c = 257.2$ with a non-dimensional wavenumber $k_c = 2.25$. Generally, the wavenumber does not depend very much on the aspect ratio. It varies only by 25% over the interval $1.05 < \Gamma < 2$. The supercritical flow consists of stationary rectangular cells that are very robust and exist for a large range of supercritical Reynolds numbers. The critical mode in an (x, z)-plane is shown over one wavelength in Figure 5. The numerical result for the critical Reynolds number is in very good agreement with the experimental value $\mathrm{Re}_c = 260$. The bifurcation is experimentally found to be supercritical. An example for a resulting pattern with four cells at Reynolds numbers $\mathrm{Re} = 750$ is shown in Figure 6. Depending on the Reynolds number history also five-cell states can be realized.

These features are very similar to those of the instability of elliptic stagnation point flow. In fact, the hyperbolic stagnation point is absent in the cat's eye state when the aspect ratio Γ is sufficiently small. Then the flow is of elliptic type and it is obvious that the instability is due to the elliptic instability mechanism. This is confirmed by the dependence of the critical Reynolds number on the aspect ratio Γ shown as a dotted line in Figure 2. When Γ is decreased to 1 the streamlines in the bulk become nearly circular and the critical Reynolds number increases sharply, because the elliptic mechanism is no longer operative.

Another argument for the elliptic mechanism is provided by the energy transfer from the basic state to the critical disturbance mode. In our calculations we observe that the energy transfer occurs mainly in the direct vicinity of the central elliptic or hyperbolic stagnation point where the flow is a superposition of rotation and straining motion. Note that the critical properties (Reynolds number, wave number) as well as the spatial distribution of the energy transfer rate change smoothly when the hyperbolic point of the base flow appears on an increase of the aspect ratio from $\Gamma = 1$. For the experimental aspect ratio $\Gamma = 1.96$ and for critical

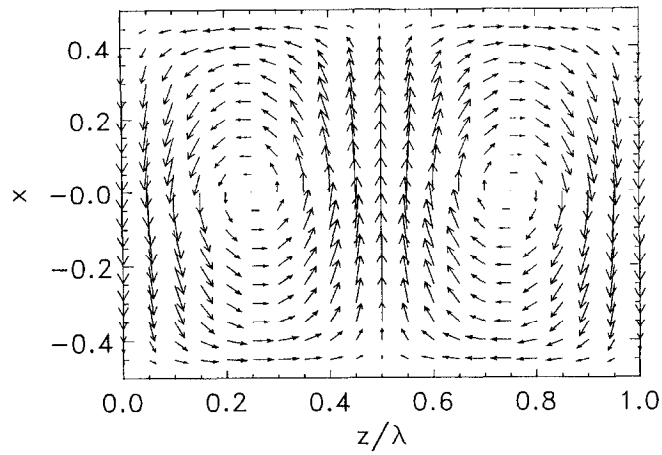

Fig. 5. – Critical mode ($k_c = 2.25$) of the cat's eye flow for $\Gamma = 1.96$ and $\mathrm{Re}_c = 257.2$ at $y = 0$. The x-axis has been scaled by d.

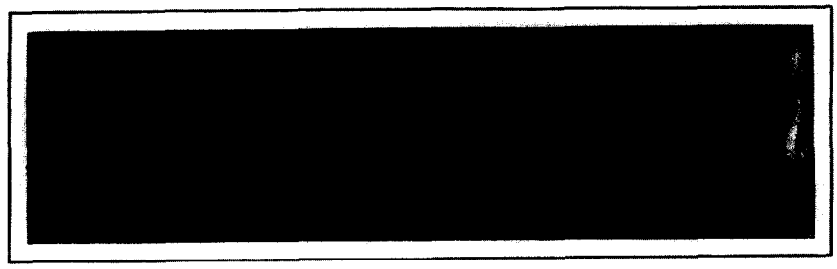

Fig. 6. – Flow pattern of a stationary four-cell state viewed from above in a layer parallel to the (x, z)-plane for $\mathrm{Re} = 750$. The flow is visualized by seeding with small amounts of aluminium flakes, using a comparatively thick light sheet at $y \approx 0$, and taking a photograph with long-time exposure (1/30 s). The field of view is slightly restricted owing to the construction of the apparatus.

conditions, about 70% of the total energy transfer between the disturbance and the base flow is carried by the destabilizing process described by the term I_2 in the energy equation (5). It describes the amplification of horizontal (x) disturbance momentum by vertical (y) advection of horizontal base state momentum similar to the so-called lift-up mechanism. The spatial distritubion of I_2 is shown in Figure 7 with a clear maximum at

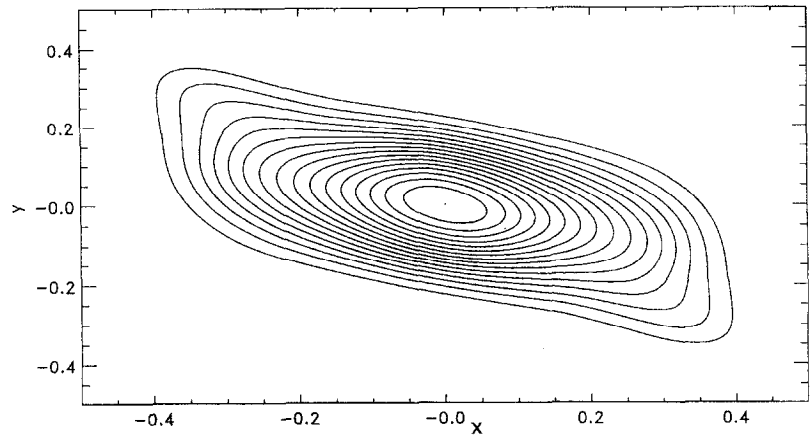

Fig. 7. – Lines of constant energy transfer rate (I_2) at criticality for $\Gamma = 1.96$ shown at the (x, y)-plane corresponding to a cell boundary ($z/\lambda = 0.5$ in Figure 5).

$x = y = 0$. Since the spatial distribution of the energy transfer rate for slightly smaller aspect ratios when the flow is purely elliptical at the center is very similar, we conclude that also for $\Gamma = 1.96$ the mechanism is essentially due to the elliptic instability process.

5. Conclusions

We have shown that the two-dimensional flow in two-sided lid-driven cavities is not unique. In particular, vortex flows with elliptic streamlines exist. As shown numerically these flows can become unstable through the elliptic instability mechanism.

The flow for the experimental aspect ratio $\Gamma = 1.96$ does possess strictly elliptical streamlines only in the centers of the two internal recirculation regions. We have presented evidence, however, that the instability of the total mixed-type flow is mainly due to the elliptic instability process. The elliptic instability can be interpreted as a resonant amplification of a standing internal wave on the vortex with elliptical streamlines. The instability of hyperbolic stagnation point flow, on the other hand, is due to vortex streching in the outgoing strain direction of the hyperbolic point. The existence of a range of parameters for which the hyperbolic stagnation point is stable in the experiment indicates that the theory for unbounded linear hyperbolic flows cannot be directly applied to the present case. For the experimental cat's eye flow the stretching leading to instability does not continue *ad infinitum* as in the linear flow case and the perturbation growth due to pure monotoneous vortex streching is limited. Rather, a perturbation amplified by a finite amount is fed back to the hyperbolic stagnation point along the stabilizing ingoing strain direction. Note that all streamlines of the basic cat's-eye flow are closed. Therefore, some resonant amplification may be possible as is typical for the elliptic process. If the three-dimensional supercritical flow patterns created as a result of the elliptic instability are robust, i.e. if they do not depend on small deviations of the base flow from elliptical, as may be evidenced by the present experimental observations, then it is natural to extend the term *elliptic instability* to more general shaped strained vortices with closed streamlines, i.e. vortices with not strictly elliptical streamlines. In this sense the present cat's-eye vortex flow seems to be capable of carrying standing inertial waves similar to those carried by the generic elliptical vortex (linear flow).

To the best of our knowledge the present result is the first experimental realization of a three-dimensional saturated flow structure in a stationary frame as a result of the elliptic instability. Previous investigations always dealt with time-dependent three-dimensional flows. In particular, Malkus (1989), in an attempt to model the tidal flow of the earth's mantle in an elliptically deformed fluid-filled cylinder, observed a periodic breakdown of the whole flow after the three-dimensional pattern reaches an appreciable amplitude. Since the present experiment also allows to observe and measure the transition to time-dependent flows, it may establish a new paradigm for the study of the elliptic instability.

Acknowledgements. – This work has been supported by the Deutsche Forschungsgemeinschaft under grant number Ku896/5-1.

REFERENCES

ALZIARY DE ROQUEFORT T., GRILLAUD G., 1978, Computation of Taylor vortex flow by a transient implicit method, *Computer Fluids*, **6**, 259.
BATCHELOR G. K., 1956, On steady laminar flow with closed streamlines at large Reynolds numbers, *J. Fluid Mech.*, **1**, 177.
BAYLY B. J., 1986, Three-dimensional instability of elliptical flow, *Phys. Rev. Lett.*, **57**, 2160.
GLEDZER E. B., PONOMAREV V. M., 1992, Instability of bounded flows with elliptical streamlines, *J. Fluid Mech.*, **240**, 1.
HERBERT Th., 1988, Secondary instability of boundary layers, *Annu. Rev. Fluid Mech.*, **20**, 487.

KELMANSON M. A., LONSDALE B., 1996, Eddy genesis in the double-lid-driven cavity, *J. Mech. Appl. Math.*, **49**, 635.

KOSEFF R. J., STREET R. L., 1984, The lid-driven cavity: a synthesis of qualitative and quantitative observations, *J.Fluids Eng.*, **106**, 390.

KÜCHEMANN D., 1965, Report on the IUTAM symposium on concentrated vortex motions in fluids, *J. Fluid Mech.*, **21**, 1.

KUHLMANN H. C., WANSCHURA M., RATH H. J., 1997, Flow in two-sided lid-driven cavities: Non-uniqueness, instabilities and cellular structures, *J. Fluid Mech.*, **336**, 267.

LAGNADO R. R., PHAN-THIEN N., LEAL L. G., 1984, The stability of two-dimensional linear flows, *Phys. Fluids*, **27**, 1094.

LANDMAN M. J., SAFFMAN P. G., 1987, The three-dimensional instability of strained vortices in a viscous fluid, *Phys. Fluids*, **30**, 2339.

LE DIZES S., ROSSI M., MOFFATT H. K., 1996, On the three-dimensional instability of elliptical vortex subjected to stretching, *Phys. Fluids*, **8**, 2084.

LIFSHITZ A., HAMEIRI E., 1991, Local stability conditions in fluid dynamics, *Phys. Fluids A*, **3**, 2644.

MALKUS W. V. R., 1989, An experimental study of global instabilities due to the tidal (elliptical) distortion of a rotating elastic cylinder, *Geophys. Astrophys. Fluid Dynamics*, **48**, 123.

MOFFATT H. K., KIDA S., OHKITANI K., 1994, Stretched vortices – the sinews of turbulence; large-Reynolds-number asymptotics, *J. Fluid Mech.*, **259**, 241.

PIERREHUMBERT R. T., 1986, Universal short-wave instability of two-dimensional eddies in an inviscid fluid, *Phys. Rev. Lett.*, **57**, 2157.

WALEFFE F., 1990, On the three-dimensional instability of strained vortices, *Phys. Fluids A*, **2**, 76.

WANSCHURA M., SHEVTSOVA V. M., KUHLMANN H. C., RATH H. J., 1995, Convective instability mechanisms in thermocapillary liquid bridges, *Phys. Fluids*, **7**, 912.

(Received 26 June 1997,
revised 02 January 1998,
accepted 05 January 1998)